Biochimica et Biophysica Acta 1777 (2008) 1195–1202

Contents lists available at ScienceDirect

Biochimica et Biophysica Acta

journal homepage: www.elsevier.com/locate/bbabio

Stepping behavior of two-headed kinesin motors

Ping Xie *

Laboratory of Soft Matter Physics, Institute of Physics, Chinese Academy of Sciences, Beijing 100080, China
Department of Physics, Renmin University of China, Beijing 100872, China

ARTICLE INFO

Article history:
Received 14 February 2008
Received in revised form 9 April 2008
Accepted 23 April 2008
Available online 1 May 2008

Keywords:
Kinesin-1
Molecular motor
Mechanochemstry
Model

ABSTRACT

The stepping behavior of the dimeric kinesin is studied by using our model based on previous biochemical, X-ray crystallography and cryo-electron microscopy studies. It is shown that, when a Pi is released from the trailing head, a forward step is made under a backward load smaller than the stall force; while when a Pi is released from the leading head, no stepping is made under a forward load or no load, and a backward step is made under a backward load. The forward stepping time, i.e., the time from the release of Pi in the trailing head to the binding of the ADP head to next binding site, is much smaller than the dwell time even under the backward load near the stall force. Thus the movement velocity of the kinesin dimer can be considered to be only dependent on ATPase rates of the two heads. The duration of the rising phase, i.e., the actual time taken by the ADP head to transit from the trailing to leading positions, is on the time scale of microseconds under any backward load smaller than the stall force. This is consistent with available experimental results.

1. Introduction

Conventional kinesin (kinesin-1) is a two-headed protein that uses the chemical energy of ATP hydrolysis to move towards the plus end of microtubule (MT) with the step size of about 8.3 nm [1–5]. A single kinesin molecule can exert maximal forces of 5–7.5 pN [6–9], can generate hundreds of steps during a single encounter with a MT [10,11], and its velocity can reach 1 μm/s at low load [9,12]. During the processive movement, the dimer occasionally steps backwards under a backward load [13–15]. When the backward load is larger than the stall force, the dimer can even move backwards stepwise in a mode of ATP-dependent processivity [15]. It is well determined that the dimer moves along MT in a hand-over-hand manner [16,17]: A given head is displaced in discrete steps with a mean size of about 17 nm [17], giving a mean step size of the dimer of about 8.3 nm.

To explain how the dimer steps and how the chemical energy is converted into the mechanical force by the dimer, a lot of models have been proposed [4,5,15–29]. The models assume that the two heads move hand-over-hand in a tightly coordinated manner, with the two heads acting dependently, which means that the two heads must somehow communicate with each other to coordinate their ATPase activity and their MT attachment and detachment. It is assumed that the conformational change in the neck-linker domain plays a crucial role in the unidirectional movement of the trailing ADP head, with the neck linker either generating a power stroke to drive the trailing ADP head moving forward [18] or acting as an irreversible switch to bias the movement of the ADP head [29].

Recently, we proposed an alternative model for the hand-over-hand movement of the dimer, in which the two heads are not tightly coordinated and the degree of coordination is dependent on the external load and mutant versus wild type [30,31]: Under a low load, the internal elastic force induces the ATPase rate of the trailing head much higher than the leading head, giving nearly one ATP molecule being hydrolyzed for making a forward step, and thus the two heads behave well coordinated. Under a large load or for some mutant kinesins even under no load, the ATPase activities of the two heads do not behave in a well-coordinated way, with more than one ATP molecule being consumed for making a forward step. Using the model, detailed analyses of various kinetic behaviors for both wild-type and a lot of mutant kinesins have been performed, which show good agreement with available experimental results. Nevertheless, the dynamics such as the stepping behavior of the dimeric kinesin during one ATPase cycle by using the model has not been quantitatively studied.

In this work, we study the stepping behavior of the dimeric kinesin by quantitatively taking into account the interaction between kinesin heads and MT, the interaction between two heads and the interaction between neck linkers and heads. The constructions of the three interactions are based on the previous biochemical and structural studies. It is shown that, when a Pi is released from the trailing head, a forward step is made even under a backward load near the stall force; while when a Pi is released from the leading head, no stepping is made under a forward load or no load, and a backward step is made under a backward load. The forward stepping time, i.e., the time from the release of Pi in the trailing head to the binding of the ADP head to next binding site, is only a few hundred microseconds even under the

* Laboratory of Soft Matter Physics, Institute of Physics, Chinese Academy of Sciences, Beijing 100080, China.
E-mail address: pxie@aphy.iphy.ac.cn.

0005-2728/$ – see front matter © 2008 Elsevier B.V. All rights reserved.
doi:10.1016/j.bbabio.2008.04.040

backward load near the stall force, which is much smaller than the dwell time (about 30 ms even at saturating ATP concentration). Thus it is a good approximation that the movement velocity of kinesin is essentially dependent only on ATPase rates of the two heads. During the forward stepping period, the duration of the rising phase, i.e., the actual time taken by the ADP head to transit from the trailing to leading positions, is on the time scale of microseconds, which is consistent with available observations in experiments [15]. It is further shown that the interaction between the two heads plays the similar role in the stepping of dimeric kinesin to the docking of the neck linker as proposed in the previous model. That is, it can reduce the forward stepping time of the trailing head and prevent the leading head from moving to the trailing position.

2. Model

Based on the previous biochemical and structural studies, we make the following assumptions to the interactions among dimeric kinesin and MT.

2.1. Interaction between a kinesin head and MT

Here we take the similar interaction potentials of a kinesin head with MT to those adopted in Xie et al. [32], which are briefly restated as follows. In nucleotide-free state the kinesin head binds strongly to MT, with the interaction potential being written as $V_S(x,y,z)=V_S^{(x)}(x)\exp[-(y-y_0)/A_y]\exp[-|z-z_0|/A_z]$ $(y\geq y_0)$, where $V_s^{(x)}(x)\leq 0$ (with the maxima equal to zero) represents the potential between the kinesin head and MT along a MT protofilament (or the longitudinal direction) and is schematically shown in Fig. 1(a). The terms $\exp[-(y-y_0)/A_y]$ and $\exp[-|z-z_0|/A_z]$ denotes the potential change in the vertical and horizontal directions, respectively, with A_y and A_z characterizing their interaction distances. Note that, due to the steric restriction of MT, the position of the kinesin head is confined to the region $y\geq y_0$. For the coordinate *oxyz* shown in Fig. 1a, we have

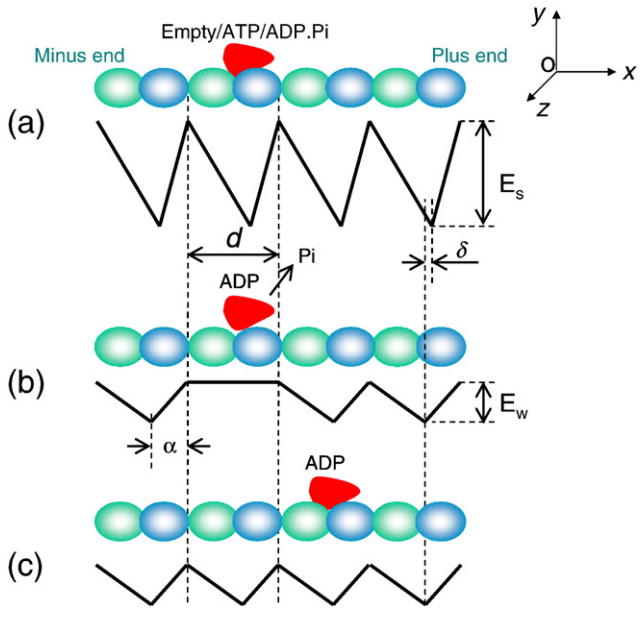

Fig. 1. Interaction potentials between a kinesin head and MT in the *x* direction (along a MT protofilament) during one ATPase cycle. (a) Strong interaction potential, $V_s^{(x)}(x)$, in nucleotide-free, ATP or ADP.Pi states. The potential depth E_s may be slightly different for the different nucleotide states. The top figure shows the position of the kinesin head relative to the MT. (b) Weak interaction potential, $V_W^{(x)}(x)$, in ADP state immediately after Pi release. The top figure shows the position of the kinesin head relative to the MT. (c) Weak interaction potential, $V_W^{(x)}(x)$, in ADP state in a period of time t_r after Pi release. The top figure shows the most probable position of the kinesin head relative to the MT.

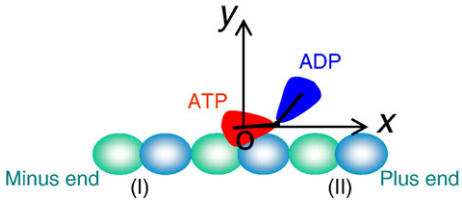

Fig. 2. Schematic diagram of the equilibrium conformation of the kinesin dimer. It is assumed that only the red head in ATP state binds strongly to MT and the blue head has no interaction with MT, e.g., by mutation Y274A/R278A/K281A in loop 12 [55,56]. (For interpretation of the references to colour in this figure legend, the reader is referred to the web version of this article.)

$y_0=z_0=0$. The potentials in the vertical and horizontal directions are similar to the Morse potential that describes the van der Waals interaction. The asymmetric potential $V_S^{(x)}(x)$ in Fig. 1a is due to the asymmetric charge distributions on the interacting surfaces of both the MT-tubulin heterodimer and kinesin head. The period of $V_S^{(x)}(x)$, $d=8.3$ nm, is equal to the distance between successive binding sites on MT.

Then ATP binding and hydrolysis occur while the kinesin head remains strongly bound to MT, with the interaction potential still being approximately described by $V_S(x,y,z)$.

Immediately after Pi release, the interaction potential becomes one that can be written as $V_W(x,y,z)=V_W^{(x)}(x)\exp[-(y-y_0)/A_y]\exp[-|z-z_0|/A_z]$ $(y\geq y_0)$, with $V_W^{(x)}(x)\leq 0$ being schematically shown in Fig. 1b. Note that, the weak-binding affinity of ADP-kinesin for MT, E_w, is smaller than the strong-binding affinity E_s of nucleotide-free, ATP-, and/or ADP.Pi-kinesin for MT [33–35]. Note also that immediately after Pi release the binding affinity of kinesin for the local binding site of MT at which the ADP.Pi-kinesin has just bound becomes even weaker than other binding sites. After a period of time, t_r, the affinity of the local binding site of MT for ADP-kinesin relaxes to the normal value and the interaction potential $V_W^{(x)}(x)$ becomes that as schematically shown in Fig. 1c. Another point to note is that, due to the different conformations near the MT-binding site of kinesin in weak and strong-binding states [36,37], the minimum position of $V_W^{(x)}(x)$ may also be slightly different from that of $V_S^{(x)}(x)$. Here, we take the minimum position of $V_S^{(x)}(x)$ is shifted by a short distance δ to the plus end of MT relative to that of $V_W^{(x)}(x)$.

The explanation to the evolution of the weak interaction potential $V_W^{(x)}(x)$ after Pi release (Figs. 1b and c) has been given in detail in Xie et al. [32]. Briefly, the conformational change in the local MT-tubulin heterodimer induced by strong binding of nucleotide-free, ATP- or ADP.Pi-kinesin [38–40] leads to a change in the charge distribution on the surface of the local tubulin, making it different from that on surfaces of other unaffected tubulins, which induces the ADP head having a further weaker interaction with the local tubulin. In a time of t_r the local tubulin heterodimer relaxes elastically to its normal conformation and, thus, the interaction potential $V_W^{(x)}(x)$ changes from that schematically shown in Fig. 1b to that shown in Fig. 1c.

2.2. Interaction between two kinesin heads

As seen from the crystal structure of dimeric kinesin determined by Kozielski et al. [41], there exists a local interaction between loop L8b from one head and loop L10 from another head. This local interaction maintains the dimer in the equilibrium conformation as schematically shown in Fig. 2. Marx et al. [42] further revealed that the dimer has this equilibrium conformation in solution. Since the two protruding loops have opposite charges, it is suggested that the local interaction is via electrostatic. Here we take this local interaction having the following form

$$V_{K-K}(x,y,z)=-V_0\ \exp\left(-\sqrt{(x-x_1)^2+(y-y_1)^2+(z-z_1)^2}/A_r\right)$$

where (x,y,z) is the center-of-mass coordinate of the ADP head relative to that of the strongly-bound head (which is taken as origin of the

coordinate, as shown in Fig. 2) during one stepping period, (x_1,y_1,z_1) is the position of ADP head in the equilibrium conformation of the dimer, $V_0>0$ is the interaction strength and A_r characterizes the interaction distance. Based upon docking of atomic structures [41] into cryo-EM images of kinesin-MT complexes [39,43] and considering that the kinesin head is approximately a sphere of radius R=2.5 nm, we approximately have $(z_1,y_1,z_1)=2R\times(\cos 20°,\sin 20°,0)$. It is noted here that, in contrast to the nucleotide-dependent binding affinity of kinesin head for MT, the interaction V_{K-K} between two heads is nucleotide independent.

2.3. Interaction between the neck linker and head

The neck linker is considered to be capable of rotating freely around its jointing point to the head. Moreover, it is assumed that the neck linker can be stretched elastically. The elastic force acting on one kinesin head induced by the stretched neck linker can be written as

$$F_{NL-K}(r) = C(r - r_0), \tag{1}$$

with the direction pointing towards the other head of the dimer, where C is the elastic coefficient, $r\equiv\sqrt{x^2+y^2+z^2}\geq r_0$ is the distance between two kinesin heads, and r_0=8 nm is the critical distance. When $r<r_0$ is within the small range (e.g., $2R\leq r<r_0$), we take $F_{NL-K}(r)=0$.

Furthermore, based on the FRET experimental results by Rice et al. [44] and the crystal structure of dimeric kinesin in ADP state [41], we make the following assumption for the effect of neck-liner docking.

When a kinesin head is in nucleotide-bound state (i.e., ATP, ADP.Pi, or ADP state), its neck linker is capable of being docked into the head domain. When the head is in nucleotide-free state, its neck linker is incapable of being docked into the head domain. In other words, the nucleotide-free state corresponds to a "closed" groove of the head domain that inhibits the neck-linker docking; while a bound nucleotide induces the groove to "open", which allows the neck-linker docking. That means that *the neck-linker docking is mainly a passive process rather than an active process*. This effect of neck-linker docking is consistent with the FRET experimental results by Rice et al. [44], where it was experimentally shown that only the nucleotide-free state corresponds to a larger mobility of the neck linker while the AMP-PNP (an analog of ATP) and ADP states to smaller motilities. It is also consistent with the determined crystal structure, showing that the neck linker is docked into the ADP head [41]. Note that this characteristic of conformational change is similar to that of the F_1-ATPase molecular motor: the close and open conformations are only dependent on nucleotide binding or not [45]. In Discuss section, we will give further discussions on the effect of neck-linker docking.

Thus when one head in nucleotide-free state binds strongly to MT, due to the incapability of its neck-linker docking, the elastic force induced by the stretched neck linker, Eq. (1), is approximately replaced by

$$F_{NL-K}(r) = C(r - r_0^*), \text{when } x\geq 2R,\ y<R \ \sin 20° \text{ and } |z|<R \tag{2a}$$

$$F_{NL-K}(r) = C(r - r_0), \text{otherwise} \tag{2b}$$

where $r_0^*<r_0$. Here we take r_0^*=5.8 nm.

2.4. Equations to describe the movement of the ADP head

With one head bound strongly to MT at position (x,y,z)=(0, 0, 0), the temporal evolution of the position of the other ADP head (relative to that of the first head) satisfies the following Langevin equations

$$\Gamma\frac{\partial x}{\partial t} = -\frac{\partial V_W(x,y,z)}{\partial x} - \frac{\partial V_{K-K}(x,y,z)}{\partial x} - F_{NL-K}(r)\frac{x}{r} + \xi_x(t), \tag{3a}$$

$$\Gamma\frac{\partial y}{\partial t} = -\frac{\partial V_W(x,y,z)}{\partial y} - \frac{\partial V_{K-K}(x,y,z)}{\partial y} - F_{NL-K}(r)\frac{y}{r} + \xi_y(t), \tag{3b}$$

$$\Gamma\frac{\partial z}{\partial t} = -\frac{\partial V_W(x,y,z)}{\partial z} - \frac{\partial V_{K-K}(x,y,z)}{\partial z} - F_{NL-K}(r)\frac{z}{r} + \xi_z(t). \tag{3c}$$

Due to the steric restriction of MT and considering the size of the kinesin head with radius R=2.5 nm, it is required that $y\geq y_0$=0 and $r\geq 2R$=5 nm. Here the drag coefficient is $\Gamma=6\pi\eta R$, where η=0.01 g cm^{-1}s^{-1} is the viscosity of the aqueous medium. $\xi_m(t)$ $(m=x, y, z)$ is the fluctuating Langevin force, with $\langle\xi_m(t)\rangle=0$ and $\langle\xi_m(t)\xi_m(t')\rangle=2k_BT\Gamma\delta_{mn}\delta(t-t')$, where k_B is the Boltzmann constant and T=300 K.

3. Results

Eq. (3) is numerically solved by using stochastic Runge–Kutta algorithm [46]. For the calculation, the following parameters are needed to be determined: the parameters related to the potentials $V_W(x,y,z)$ and $V_S(x,y,z)$, i.e., α, E_w, E_s, A_y and A_z, the parameters related to the potential $V_{K-K}(x,y,z)$, i.e., V_0 and A_r, and the parameters related to the neck linkers, i.e., δ and C. For the parameters related to the potentials $V_W(x,y,z)$ and $V_S(x,y,z)$, we take α=3 nm, $E_w=13k_BT$, $E_s=25k_BT$, $A_y=A_z$=2 nm. These values of α, E_w, E_s, A_y and A_z are the same as those used in Xie et al. [32] that have been fitted to the experimental results on single-headed kinesin KIF1A [47,48]. Moreover, we have checked that, by varying the value of E_w from $12k_BT$ to $16k_BT$, we obtained the very similar results. As anticipated, the results are not sensitive to E_s provided that it is very large and, also, the results are insensitive to values of A_y, A_z, and α. For the parameter related to the neck linkers, the results are independent of the individual values of δ and C, provided that their product gives the value that is close to the internal elastic force due to the stretching of neck linker when two heads are simultaneously bound strongly to MT (rigor state). In the calculation we take δ=0.3 nm C=12 pN/nm, which give the internal elastic force as $F_{NL-K}(r)$=3.6 pN that is close to those used before [30,31,49]. For the parameters related to the potential $V_{K-K}(x,y,z)$, we take A_r=2 nm that is the same as that of A_y or A_z. Moreover, we have checked that the variation of the value of A_r has no sensitive effect on the calculated results. Thus, only one parameter V_0 is left, which either is unavailable from previous experimental results or has the sensitive effect on the calculated results. Therefore, we will take it as an adjustable parameter in this work. Except in section 3.3, where we will study the effect of V_0 on the stepping behavior by varying V_0, throughout we take $V_0=13k_BT$.

In addition, to satisfy the requirements of $y\geq y_0$ and $r\geq 2R$, in the calculation we add a constant force of 30 pN pointing towards the normal direction of the contacting surface whenever $y<y_0$ or $r<2R$.

3.1. Stepping without the external load

Based on the model we proposed before [30,31], in rigor state with both heads bound strongly to MT the dimeric kinesin can be in either of the two states as shown in Fig. 3, where in Fig. 3a the trailing head is in ATP or ADP.Pi state and the leading head is in ATP or ADP.Pi state, while in Fig. 3b the trailing head is in ATP or ADP.Pi state and the leading head is nucleotide free. The release of a Pi may induce the

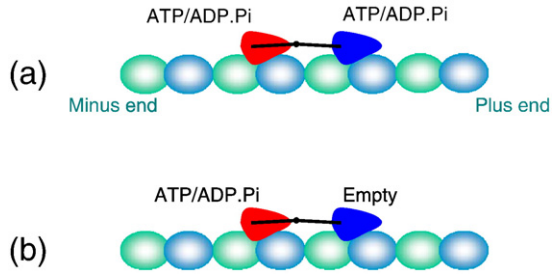

Fig. 3. Two possible rigor states with both heads bound strongly to MT. (a) The trailing head is in either ATP or ADP.Pi state and the leading head is in either ATP or ADP.Pi state. (b) The trailing head is in either ATP or ADP.Pi state and the leading head is in nucleotide-free state.

movement of kinesin. In the two rigor states as shown in Fig. 3 the Pi release can occur in three cases: (i) The Pi release occurs from the trailing head while the leading head is in ATP or ADP.Pi state. (ii) The Pi release occurs from the leading head while the trailing head is in ATP or ADP.Pi state. (iii) The Pi release occurs from the trailing head while the leading head is in nucleotide-free state, which often occurs at low ATP concentration. In the following we study the stepping behavior induced by a Pi release in the three cases separately.

First, consider that the Pi release from the trailing (red) head occurs before from the leading (blue) head (see top figure in Fig. 4). Fig. 4 shows a typical result for the temporal evolution of the position of the red head relative to the blue head bound strongly to MT at position (0, 0, 0). Here it is set that the Pi is released from the red head at $t=0$ and the ADP is released from the red head at $t=20$ μs. Note that the blue head is in ATP or ADP.Pi state, which implies that its neck linker can be docked into the head domain. It is seen that, after Pi release, the trailing (red) head rapidly becomes the leading one. After becoming the leading head and before ADP releasing from it, due to its weak interaction with MT, the ADP head is not fixed at the position of the kinesin-MT interaction potential minimum ($x=8$ nm, $y=0$), while occasionally moves backwards to the position of the head-head interaction potential minimum ($x=5\cos 20^\circ \approx 4.7$ nm, $y=5\sin 20^\circ \approx 1.71$ nm). After ADP is released, the nucleotide-free head becomes bound strongly to MT, fixed at the position of the kinesin-MT interaction potential minimum ($x=8.3$ nm, $y=0$).

Then consider that the Pi release from the leading (blue) head occurs before from the trailing (red) head (see top figure in Fig. 5). A typical result for the temporal evolution of the position of the blue head relative to the red head in ATP or ADP.Pi state bound strongly to MT at position (0, 0, 0) is shown in Fig. 5. Here it is set that the Pi is released from the blue head at $t=0$, the affinity of the local binding site of MT for ADP head relaxes to the normal value at $t=100$ μs and the ADP is released from the blue head at $t=200$ μs after it rebinds to MT. It is seen that after Pi release the leading head rapidly moves to and then

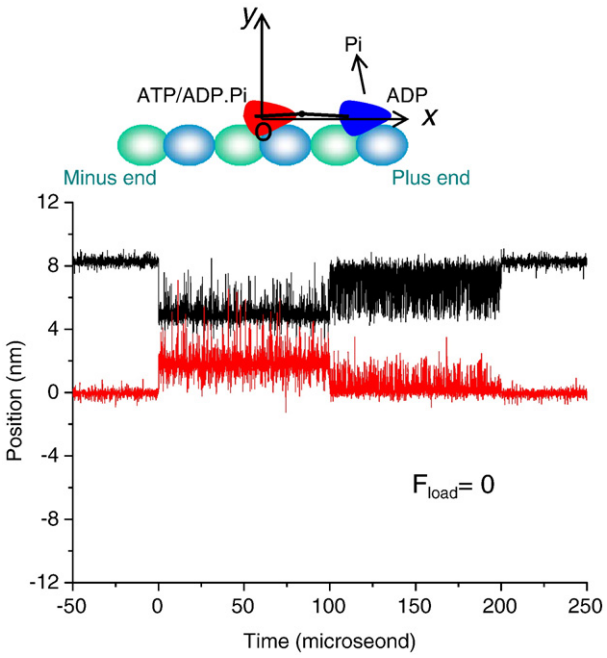

Fig. 5. A calculated result for the temporal evolution of the position of the blue head relative to the red head in ATP or ADP.Pi state bound strongly to MT at position (0, 0, 0) under no external load. The Pi is released from the red head occurring at $t=0$. It is taken that after $t_r=100$ μs the affinity of the local binding site of MT for ADP-kinesin relaxes to the normal value and at $t=200$ μs the ADP is released from the blue head after it rebinds to MT. Black and red curves are for the x and y components, respectively. For clarity, the result for the z component is not shown here. The top figure shows schematically the positions of the two heads at $t=0$.

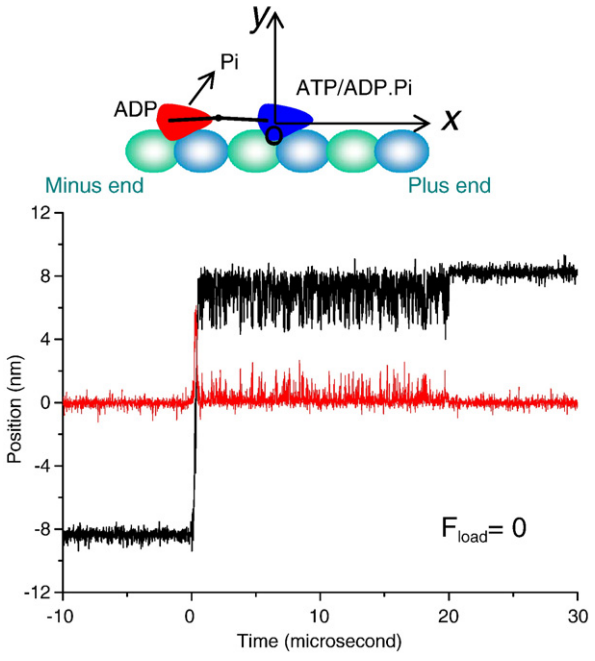

Fig. 4. A calculated result for the temporal evolution of the position of the red head relative to the blue head in ATP or ADP.Pi state bound strongly to MT at position (0, 0, 0) under no external load. The Pi is released from the red head occurring at $t=0$ and the ADP is released from the red head occurring at $t=20$ μs. Black and red curves are for the x and y components, respectively. For clarity, the result for the z component is not shown here. The top figure shows schematically the positions of the two heads at $t=0$.

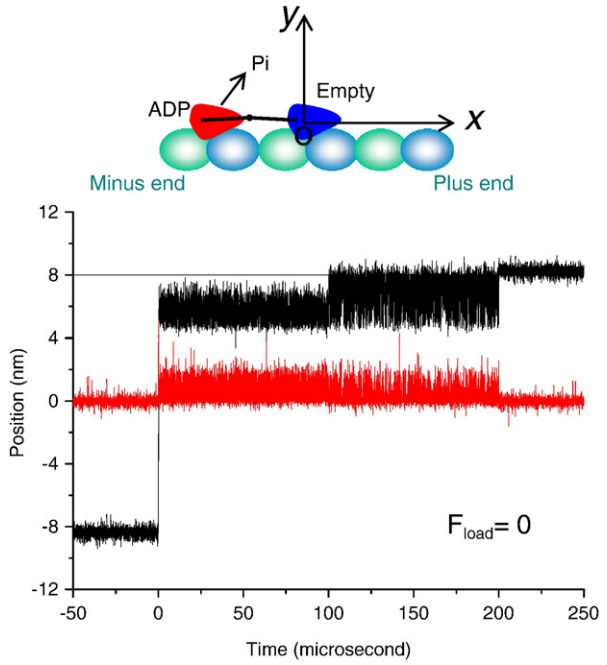

Fig. 6. A calculated result for the temporal evolution of the position of the red head relative to the blue head in nucleotide-free state bound strongly to MT at position (0, 0, 0) under no external load. The Pi is released from the red head occurring at $t=0$. It is taken that at $t=100$ μs an ATP binds to the blue head and at $t=200$ μs the ADP is released from the red head. Black and red curves are for the x and y components, respectively. For clarity, the result for the z component is not shown here. The top figure shows schematically the positions of the two heads at $t=0$.

stays at the position of the head-head interaction potential minimum ($x \approx 4.7$ nm, $y \approx 1.71$ nm). This is due to that there exists no interaction of the ADP head with the local binding site of MT and the interaction between the two heads prevents the ADP head from moving backwards further to become the trailing one. After the local MT-tubulin heterodimers relaxes to the normal conformations, the ADP head becomes able to rebind to MT at position ($x=8$ nm, $y=0$), thus triggering MT-activated ADP release. After ADP is released, the nucleotide-free head becomes bound strongly to MT, fixed at the position of the kinesin-MT interaction potential minimum ($x=8.3$ nm, $y=0$).

Third, consider that Pi release occurs in the trailing (red) head while the leading (blue) head is nucleotide free (see top figure in Fig. 6). A typical result for the temporal evolution of the position of the red head relative to the blue head bound strongly to MT at position (0, 0, 0) is shown in Fig. 6. Here it is set that the Pi is released from the red head at $t=0$ and an ATP binds to the blue head at $t=100$ μs. It is seen that, because the neck linker of the blue head in nucleotide-free state cannot be docked before $t=100$ μs, the red head cannot be bound appropriately to MT at position ($x=8$ nm, $y=0$) after the red head becomes the leading one, thus prohibiting ADP release. This is consistent with Alonso et al. [50] and the experimental observation by Hackney [51]. Once an ATP binding to the blue head at $t=100$ μs, its neck linker becomes able to be docked and the red leading head can be bound appropriately to MT at position ($x=8$ nm, $y=0$), thus triggering MT-activated ADP release. After ADP release occurred at $t=200$ μs, the nucleotide-free head becomes bound strongly to MT, fixed at the position of the kinesin-MT interaction potential minimum ($x=8.3$ nm, $y=0$).

Thus from Figs. 4–6 we see that, under no external load, when a Pi is released from the trailing head a forward step is made, implying an effective mechanochemical coupling; while when a Pi is released from

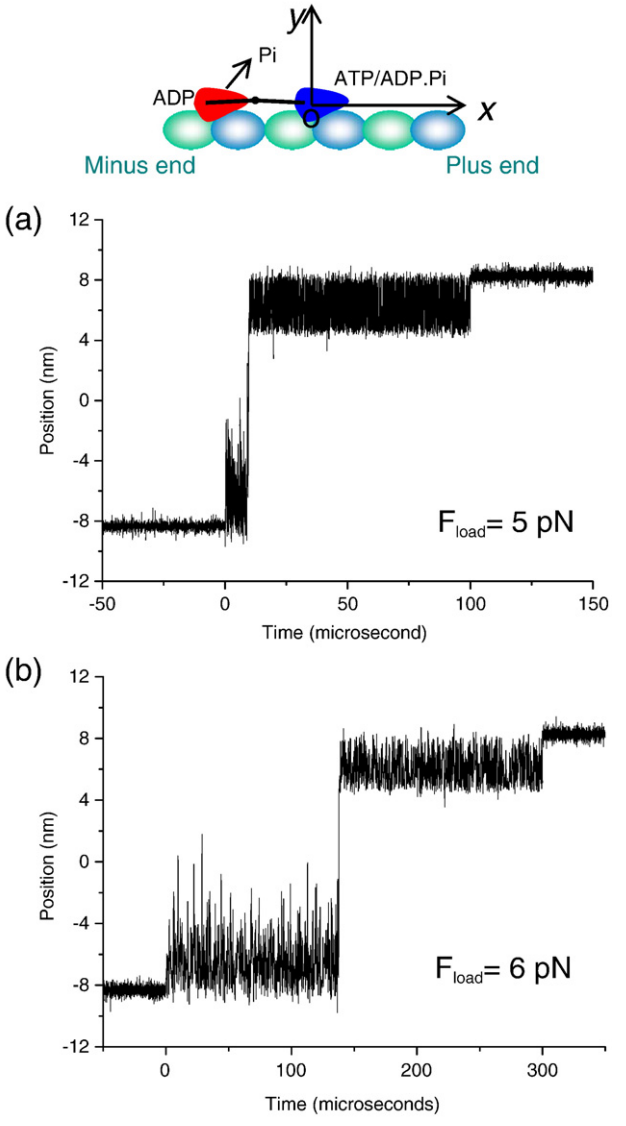

Fig. 7. Results for the temporal evolution of the position of the red head relative to the blue head bound strongly to MT at position (0, 0, 0) under the external load F_{load} The Pi is released from the red head occurring at $t=0$. (a) $F_{load}=5$ pN. The ADP is released from the red head at $t=100$ μs. (b) $F_{load}=6$ pN. The ADP is released from the red head at $t=300$ μs. For clarity, only the results for the x component are shown here. The top figure shows schematically the positions of the two heads at $t=0$.

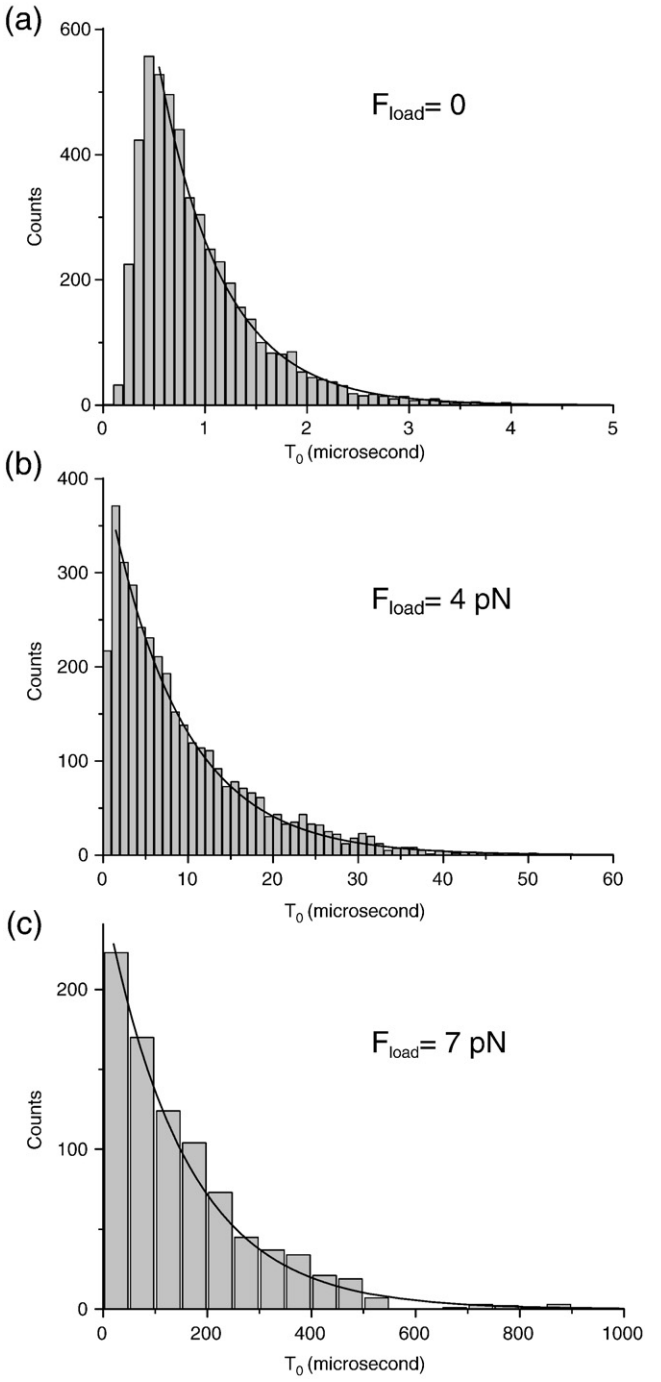

Fig. 8. Distributions of the first-passage time T_0 for the trailing head to become the leading one under external load $F_{load}=0$ (a), $F_{load}=4$ pN (b) and $F_{load}=7$ pN (c). The lines are exponential fittings.

the leading head neither a forward nor a backward step is made, implying a futile mechnochemical coupling. Since in rigor state with both heads bound strongly to MT, due to the internal elastic force resulted from the stretching of the neck linkers, the Pi-release rate of the trailing head is enhanced while that of the leading head is greatly reduced for the wild-type kinesin dimer [31,49], resulting in the rare occurrence of the futile mechanochemical coupling and thus nearly one ATP being hydrolyzed per step (nearly 1:1 coupling). Therefore, the two heads of the wild-type kinesin dimer under no external load behaves well coordinated in their mechanochemical couplings, which is consistent with the previous experiments.

3.2. Stepping with the external load

To study the effect of an external load F_{load} on the stepping behavior, we simply add a constant force $-F_{load}/2$ on the right-hand side of Eq. (3a), while the other half of the external load, $-F_{load}/2$, is acting on another head that is bound strongly to MT. Here F_{load} is defined as positive when it is pointed towards the minus end of MT.

In Fig. 7 we show two typical results for the temporal evolution of the position of the red head relative to the blue head bound strongly to MT at position (0, 0, 0) (see top figure in Fig. 7) for different values of F_{load}. Here it is set that the release of Pi from the red head occurs at $t=0$ and the release of ADP from the red head occurs at $t=100$ μs in Fig. 7a and occurs at $t=300$ μs in Fig. 7b. It is seen that, as anticipated, the backward load F_{load} increases the time, T_0, taken by the trailing head to become the leading one after the Pi is released from it. Here T_0 is defined as the first-passage time for the red head to reach position ($x=8$ nm, $y=0$, $z=0$) after the release of Pi. An interesting point to note from Fig. 7 is that, although the time T_0 defined in this work is increased by the backward load, the duration of the rising phase, i.e., the actual time taken by the red head to change from the trailing to leading positions, is nearly independent of the load and is very short (a few microseconds). This implies that in experiments one will always observe a very short duration of the rising phase even with a large backward load, which is consistent with the previous experimental observations [15].

To further study the effect of load on T_0, in Fig. 8 we show the distribution of T_0 for several different values of loads. It is seen that, as the load increases, both the mean value of T_0 and the breadth of its distribution increase. Except in the region of very small T_0, the distributions can be fitted well exponentially. From Fig. 8c, we see that even near the stall force (e.g., at load $F_{load}=7$ pN), the probability for the occurrence of $T_0>1$ ms is negligibly small. In Fig. 9 we show the mean value of T_0, $\langle T_0\rangle$, versus load F_{load} by filled circles. It is seen that

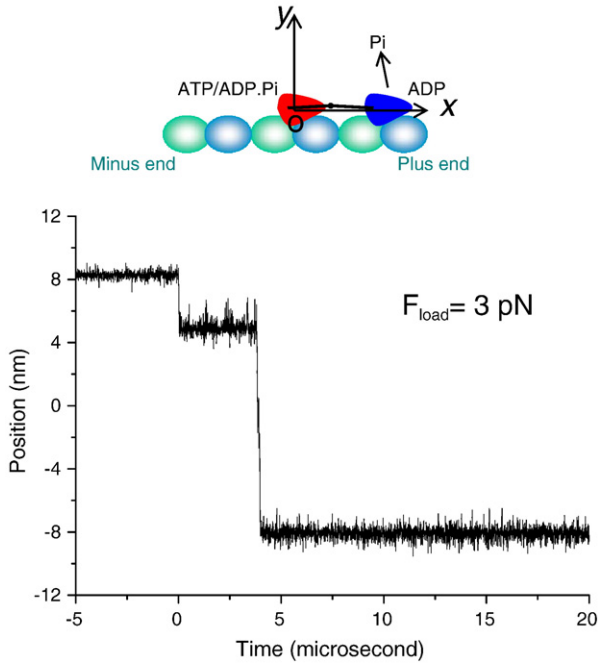

Fig. 10. A calculated result for the temporal evolution of the position of the blue head relative to the red one bound strongly to MT at position (0, 0, 0) under external load $F_{load}=3$ pN. The Pi is released from the red head occurring at $t=0$. Here only the result for the x component is shown. The top figure shows schematically the positions of the two heads at $t=0$.

under low loads, i.e., $F_{load}\leq 4$ pN, $\langle T_0\rangle$ is smaller than 10 μs. Even near the stall force, $\langle T_0\rangle$ is smaller than 200 μs.

Thus the stepping of kinesin during its processive movement is a very fast process. Since the stepping time or the mean first-passage time $\langle T_0\rangle$ is much shorter than the dwell time t_{dwell} (e.g., even under saturating ATP concentration, $t_{dwell}=k_2^{-1}+k_3^{-1}=30$ ms, where the ATP-hydrolysis rate $k_2=100$ s^{-1} and Pi-release rate $k_3=50$ s^{-1} [23]), it is a good approximation that the movement velocity of kinesin is essentially dependent only on ATPase rates of the two heads. Indeed, as we have shown elsewhere [30,31], the theoretical results of the mean velocity, which were obtained based solely on the ATPase rates of the two heads, versus [ATP], [ADP], [Pi], temperature, external load, different mutations, etc., show good quantitative agreement with available experimental results.

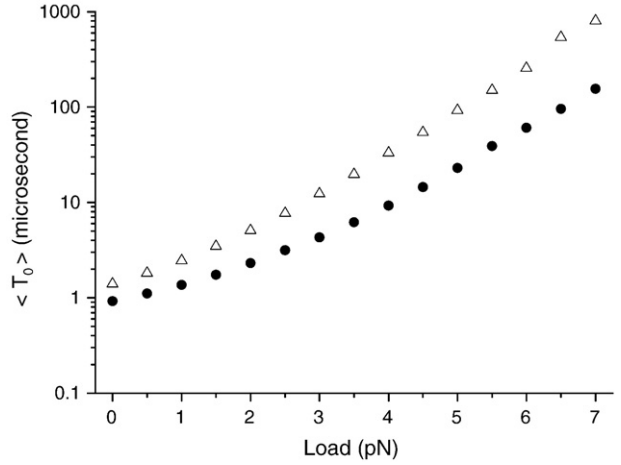

Fig. 9. Mean first-passage time $\langle T_0\rangle$ for the trailing head to become the leading one versus external load F_{load}. The filled circles and unfilled triangles are the results with and without the consideration of the interaction between two heads, respectively.

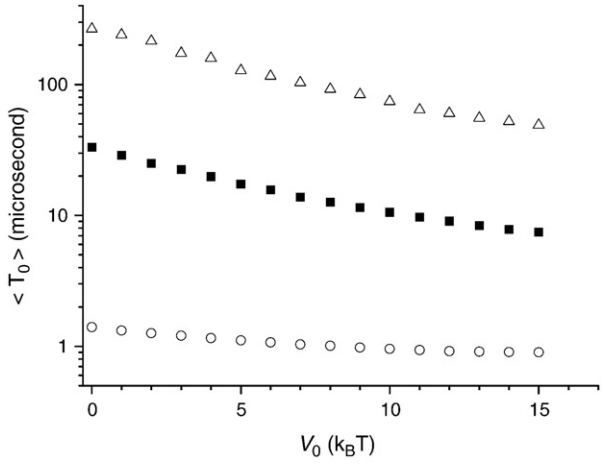

Fig. 11. The V_0 dependence of the mean first-passage time taken by the trailing head to become the leading one after the Pi is released from it under external load $F_{load}=0$ (unfilled circles), $F_{load}=4$ pN (filled squares) and $F_{load}=6$ pN (unfilled triangles).

As seen in Fig. 5, under no load, after a Pi is released from the leading head, no stepping is made. However, an intermediate or high backward load together with the thermal noise can overcome the interaction between two heads, resulting in the backward stepping after a Pi is released from the leading head. A typical result for the temporal evolution of the position of the blue head relative to the red one bound strongly to MT at position (0, 0, 0) (see top figure in Fig. 10) is shown in Fig. 10. Here it is set that the Pi is released from the blue head at $t=0$. Thus, it is concluded that when a Pi is released from the trailing head a forward step will be made; while, under the case of a backward load that is not very low, when a Pi is released from the leading head a backward step will be made. In other words, under the case of the backward load, the direction of stepping of dimeric kinesin is determined by whether a Pi is released from the trailing head or from the leading head. Indeed, as it has been demonstrated before [31], the backward stepping behavior that were obtained based on this argument show good quantitative agreement with previous experimental results [13–15].

3.3. Effect of interaction between two heads on the stepping behavior

If there is no interaction between the two heads, i.e., taking $V_0=0$, it is noted that after a Pi is released from the trailing head the kinesin can still make a forward step. However, the stepping time will be increased as compared with that in the presence of the interaction between the two heads. This can be seen in Fig. 9, where the mean first-passage time $\langle T_0\rangle$ versus the external load under $V_0=0$ are shown by unfilled triangles. As backward load increases, the reduction of the stepping time $\langle T_0\rangle$ due to the interaction between two heads becomes more pronounced. To see the effect of V_0 on the stepping behavior, in Fig. 11 we show the stepping time $\langle T_0\rangle$ as a function of V_0 for different backward loads. It is seen that, for a given backward load, $\langle T_0\rangle$ decreases with the increase of V_0, which is more pronounced for small values of V_0. For large values of V_0, the decrease of $\langle T_0\rangle$ with V_0 becomes not pronounced.

Moreover, to see the effect of V_0 on the backward stepping behavior, in Fig. 12 we show the V_0 dependence of the mean first-passage time $\langle T_0\rangle$ taken by the leading head to become the trailing one after the Pi is released from it under no load (filled triangles). For comparison, in the figure we also show the mean first-passage time $\langle T_0\rangle$ taken by the trailing head to become the leading one after the Pi is released from it (unfilled circles). It is seen that, as V_0 increases, the backward stepping time increases significantly, in contrast to the forward stepping time that decreases with the increase of V_0. Thus the large value of V_0 can prevent the leading head from moving to the trailing position.

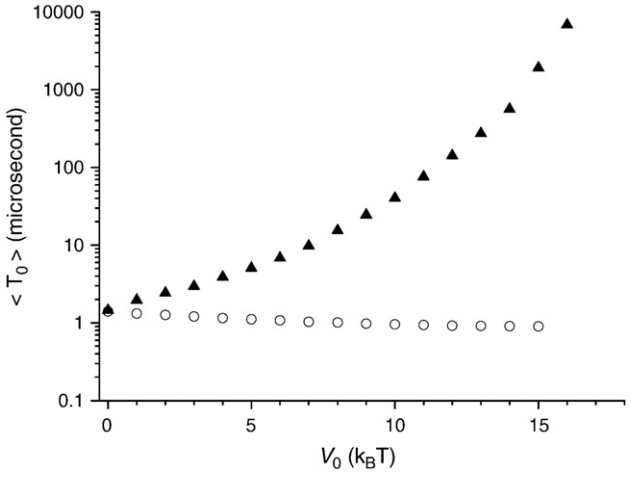

Fig. 12. Effect of V_0 on stepping time under no load. Filled triangle are the results for the mean first-passage time taken by the leading head to become the trailing one after the Pi is released from it, while unfilled circles are the results for the mean first-passage time taken by the trailing head to become the leading one after the Pi is released from it.

Therefore, the strong interaction between the two heads can reduce the forward stepping time of the trailing head after a Pi is released from it and prevent the leading head from moving to the trailing position after a Pi is released from it under case of no or forward load.

4. Discussion

In this work, the stepping behavior of dimeric kinesin under various conditions is quantitatively studied by using our proposed model. It is shown that a forward stepping is gated by a Pi release from the trailing (or rear) head. As we have discussed in detail in the Supplementary materials of Xie et al. [49], this is consistent with the experiment on kinesin backsteps induced by nucleotide analogs reported in Guydosh and Block [52], where, however, the authors had proposed that "the front head of kinesin is gated".

The interaction between the two heads proposed here plays the similar role in the forward stepping of the trailing head to the docking of the neck linker into the strongly bound leading head as proposed in the previous model [18]. (i) In the present model, the interaction between the two heads reduces the forward stepping time of the detached ADP head; while the neck-liner docking in the previous model drives directly the forward movement of the ADP head. (ii) The interaction between the two heads has the same effect as the docking of neck linker to prevent the weakly bound ADP head in the leading position from moving to the trailing position. However, the main distinction between the two arguments is that in the present model the docking of neck linker is mainly a passive process, which is mainly induced by the interaction between the two heads; while in the previous model the docking of neck linker is an active process. Thus, in the former, the free-energy change associated with the neck-liner immobilization (docking) of a truncated single kinesin head is small. However, the interaction-induced transition of the dimer from conformation in rigor state to the equilibrium conformation as shown in Fig. 2, which is associated with the transition of the neck liner from the undocking to docking states, accompanies a large free-energy change. These are consistent with the experimental results by Rice et al. [53], showing that for a truncated single kinesin head the free-energy change associated with neck-linker immobilization (docking) is small. They are also consistent with the experiment of Hackney [54], showing that for a two-headed kinesin the free-energy change associated with the neck-linker docking can, however, be large. Moreover, it is noted that the large value of V_0 predicted in this work is consistent with the experimental results that a significant fraction of the free energy of ATP hydrolysis, which is about $23k_BT$, is available to drive the docking of the neck linker [54]. In the latter model, since the neck-liner docking is an active process, in order to overcome a large backward load so as to prevent the weakly bound ADP head in the leading position from moving to the trailing position, the free-energy change associated with neck-liner docking should be large. This is inconsistent with the experimental results by Rice et al. [53].

In the present model, the unidirectional movement of kinesin is realized by two asymmetric interactions: (i) One is the interaction between two heads. As seen in Fig. 2, the position of the detached ADP head, at which it has the strongest interaction with another head that is strongly bound to MT, is asymmetric relative to the two binding sites (I) and (II) on MT. Thus, even the two binding sites (I) and (II) have the same binding affinity for the detached ADP head and the two heads have the same ATPase rate, the asymmetric interaction will provide different binding probabilities to sites (I) and (II), giving rise to the unidirectional movement. (ii) Immediately after Pi release the binding affinity of binding site (II) for ADP head is different from that of site (I) for ADP head. Thus, even there is no interaction between two heads and the two heads have the same ATPase rate, the different binding affinities result in different binding probabilities to sites (I) and (II), giving rise to the unidirectional movement.

References

[1] J. Howard, The movement of kinesin along microtubules, Annu. Rev. Physiol. 58 (1996) 703–729.
[2] N. Hirokawa, Kinesin and dynein superfamily proteins and the mechanism of organelle transport, Science 279 (1998) 519–526.
[3] R.D. Vale, The molecular motor toolbox for intracellular transport, Cell 112 (2003) 467–480.
[4] R.A. Cross, The kinetic mechanism of kinesin, Trends Biochem. Sci. 29 (2004) 301–309.
[5] C.L. Asbury, Kinesin: world's tiniest biped, Curr. Opin. Cell Biol. 17 (2005) 89–97.
[6] K. Svoboda, S.M. Block, Force and velocity measured for single kinesin molecules, Cell 77 (1994) 773–784.
[7] E. Meyhöfer, J. Howard, The force generated by a single kinesin molecule against an elastic load, Proc. Natl. Acad. Sci. U. S. A. 92 (1995) 574–578.
[8] C.M. Coppin, D.W. Pierce, L. Hsu, R.D. Vale, The load dependence of kinesin's mechanical cycle, Proc. Natl. Acad. Sci. U. S. A. 94 (1997) 8539–8544.
[9] K. Visscher, M.J. Schnitzer, S.M. Block, Single kinesin molecules studied with a molecular force clamp, Nature 400 (1999) 184–189.
[10] J. Howard, A.J. Hudspeth, R.D. Vale, Movement of microtubules by single kinesin molecules, Nature 342 (1989) 154–158.
[11] S.M. Block, L.S. Goldstein, B.J. Schnapp, Bead movement by single kinesin molecules studied with optical tweezers, Nature 348 (1990) 348–352.
[12] W. Hua, E.C. Young, M.L. Fleming, J. Gelles, Coupling of kinesin steps to ATP hydrolysis, Nature 388 (1997) 390–393.
[13] M. Nishiyama, H. Higuchi, T. Yanagida, Chemomechanical coupling of the ATPase cycle to the forward and backward movements of single kinesin molecules, Nat. Cell Biol. 4 (2002) 790–797.
[14] Y. Taniguchi, M. Nishiyama, Y. Ishii, T. Yanagida, Entropy rectifies the Brownian steps of kinesin, Nat. Chem. Biol. 1 (2005) 342–347.
[15] N.J. Carter, R.A. Cross, Mechanics of the kinesin step, Nature 435 (2005) 308–312.
[16] C.L. Asbury, A.N. Fehr, S.M. Block, Kinesin moves by an asymmetric hand-over-hand mechanism, Science 302 (2003) 2130–2134.
[17] A. Yildiz, M. Tomishige, R.D. Vale, P.R. Selvin, Kinesin walks hand-over-hand, Science 303 (2004) 676–678.
[18] R.D. Vale, R.A. Milligan, The way things move: looking under the hood of molecular motor proteins, Science 288 (2000) 88–95.
[19] A. Yildiz, P.R. Selvin, Kinesin: walking, crawling or sliding along? Trends Cell Biol. 15 (2005) 112–120.
[20] C.S. Peskin, G. Oster, Coordinated hydrolysis explains the mechanical behavior of kinesin, Biophys. J. 68 (1995) 202s–210s.
[21] T. Duke, S. Leibler, Motor protein mechanics: a stochastic model with minimal mechanochemical coupling, Biophys. J. 71 (1996) 1235–1247.
[22] E. Mandelkow, K.A. Johnson, The structural and mechanochemical cycle of kinesin, Trends Biochem. Sci. 23 (1998) 429–433.
[23] S.P. Gilbert, M.L. Moyer, K.A. Johnson, Alternating site mechanism of the kinesin ATPase, Biochemistry 37 (1998) 792–799.
[24] W.O. Hancock, J. Howard, Kinesin's processivity results from mechanical and chemical coordination between the ATP hydrolysis cycles of the two motor domains, Proc. Natl. Acad. Sci. U. S. A. 96 (1999) 13147–13152.
[25] S.A. Endow, D.S. Barker, Processive and nonprocessive models of kinesin movement, Annu. Rev. Physiol. 65 (2003) 161–175.
[26] L.M. Klumpp, A. Hoenger, S.P. Gilbert, Kinesin's second step, Proc. Natl. Acad. Sci. U. S. A. 101 (2004) 3444–3449.
[27] S.S. Rosenfeld, P.M. Fordyce, G.M. Jefferson, P.H. King, S.M. Block, Stepping and stretching: how kinesin uses internal strain to walk processively, J. Biol. Chem. 278 (2003) 18550–18556.
[28] Q. Shao, Y.Q. Gao, On the hand-over-hand mechanism, Proc. Natl. Acad. Sci. U. S. A. 103 (2006) 8072–8077.
[29] R.F. Fox, M.H. Choi, Rectified Brownian motion and kinesin motion along microtubules, Phys. Rev. E 63 (2001) 051901.
[30] P. Xie, S.-X. Dou, P.-Y. Wang, Model for kinetics of wild-type and mutant kinesins, Biosystems 84 (2006) 24–38.
[31] P. Xie, S.-X. Dou, P.-Y. Wang, Mechanochemical couplings of kinesin motors, Biophys. Chem. 123 (2006) 58–76.
[32] P. Xie, S.-X. Dou, P.-Y. Wang, Processivity of single-headed kinesin motors, Biochim. Biophys. Acta 1767 (2007) 1418–1427.
[33] I.M. Crevel, A. Lockhart, R.A. Cross, Weak and strong states of kinesin and ncd, J. Mol. Biol. 257 (1996) 66–76.
[34] S. Uemura, K. Kawaguchi, J. Yajima, M. Edamatsu, Y.Y. Toyoshima, S. Ishiwata, Kinesin-microtubule binding is dependent on both nucleotide state and loading direction, Proc. Natl. Acad. Sci. U. S. A. 99 (2002) 5977–5981.
[35] R. Nitta, M. Kikkawa, Y. Okada, N. Hirokawa, KIF1A alternately uses two loops to bind microtubules, Science 305 (2004) 678–683.
[36] M. Kikkawa, E.P. Sablin, Y. Okada, H. Yajima, R.J. Fletterick, N. Hirokawa, Switch based mechanism of kinesin motors, Nature 411 (2001) 439–445.
[37] B.J. Grant, J.A. McCammon, L.S.D. Caves, R.A. Cross, Multivariate analysis of conserved sequence–structure relationships in kinesins: coupling of the active site and a tubulin-binding sub-domain, J. Mol. Biol. 368 (2007) 1231–1248.
[38] A. Hoenger, E.P. Sablin, R.D. Vale, R.J. Fletterick, R.A. Milligan, Three-dimensional structure of a tubulin–motor–protein complex, Nature 376 (1995) 271–274.
[39] A. Hoenger, R.A. Milligan, Motor domains of kinesin and ncd interact with microtubule protofilaments with the same binding geometry, J. Mol. Biol. 265 (1997) 553–564.
[40] K. Hirose, W.B. Amos, A. Lockhart, R.A. Cross, L.A. Amos, Three-dimensional cryoelectron microscopy of 16-protofilament microtubules: structure, polarity, and interaction with motor proteins, J. Struct. Biol. 118 (1997) 140–148.
[41] F. Kozielski, S. Sack, A. Marx, M. Thormahlen, E. Schonbrunn, V. Biou, A. Thompson, E.-M. Mandelkow, E. Mandelkow, The crystal structure of dimeric kinesin and implications for microtubule-dependent motility, Cell 91 (1997) 985–994.
[42] A. Marx, M. Thormählen, J. Müller, S. Sack, E.-M. Mandelkow, E. Mandelkow, Conformations of kinesin: solution vs. crystal structures and interactions with microtubules, Eur. Biophys. J. 27 (1998) 455–465.
[43] H. Sosa, D.P. Dias, A. Hoenger, M. Whittaker, E. Wilson-Kubalek, E. Sablin, R.J. Fletterick, R.D. Vale, R.A. Milligan, A model for the microtubule-Ncd motor protein complex obtained by cryo-electron microscopy and image analysis, Cell 90 (1997) 217–224.
[44] S. Rice, A.W. Lin, D. Safer, C.L. Hart, N. Naber, B.O. Carragher, S.M. Cain, E. Pechatnikova, E.M. Wilson-Kubalek, M. Whittaker, E. Pate, R. Cooke, E.W. Taylor, R.A. Milligan, R.D. Vale, A structural change in the kinesin motor protein that drives motility, Nature 402 (1999) 778–784.
[45] J. Abrahams, A. Leslie, R. Lutter, J. Walker, Structure at 2.8 Å resolution of F1-ATPase from bovine heart mitochondria, Nature 370 (1994) 621–628.
[46] R.L. Honeycutt, Stochastic Runge–Kutta algorithms. I. White noise, Phys. Rev. A 45 (1992) 600–603.
[47] Y. Okada, N. Hirokawa, Mechanism of the single-headed processivity: Diffusional anchoring between the K-loop of kinesin and the C terminus of tubulin, Proc. Natl. Acad. Sci. U. S. A. 97 (2000) 640–645.
[48] Y. Okada, H. Higuchi, N. Hirokawa, Processivity of the single-headed kinesin KIF1A through biased binding to tubulin, Nature 424 (2003) 574–577.
[49] P. Xie, S.-X. Dou, P.-Y. Wang, Limping of homodimeric kinesin motors, J. Mol. Biol. 366 (2007) 976–985.
[50] M.C. Alonso, D.R. Drummond, S. Kain, J. Hoeng, L. Amos, R.A. Cross, An ATP gate controls tubulin binding by the tethered head of kinesin-1, Science 316 (2007) 120–123.
[51] D.D. Hackney, Evidence for alternating head catalysis by kinesin during microtubule-stimulated ATP hydrolysis, Proc. Natl. Acad. Sci. U. S. A. 91 (1994) 6865–6869.
[52] N.R. Guydosh, S.M. Block, Backsteps induced by nucleotide analogs suggest the front head of kinesin is gated by strain, Natl. Acad. Sci. U. S. A. 103 (2006) 8054–8059.
[53] S. Rice, Y. Cui, C. Sindelar, N. Naber, M. Matuska, R. Vale, R. Cooke, Thermodynamic properties of the kinesin neck region docking to the catalytic core, Biophys. J. 84 (2003) 1844–1854.
[54] D.D. Hackney, The tethered motor domain of a kinesin-microtubule complex catalyzes reversible synthesis of bound ATP, Proc. Natl. Acad. Sci. U. S. A. 102 (2005) 18338–18343.
[55] G. Woehlke, A.K. Ruby, C.L. Hart, B. Ly, N. Hom-Booher, R.D. Vale, Microtubule interaction site of the kinesin motor, Cell 90 (1997) 207–216.
[56] K. Kaseda, H. Higuchi, K. Hirose, Coordination of kinesin's two heads studied with mutant heterodimers, Proc. Natl Acad. Sci. U. S. A. 99 (2002) 16058–16063.